Author's Accepted Manuscript

GYY4137, a slow-releasing hydrogen sulfide donor, ameliorates renal damage associated with chronic obstructive uropathy

S. Lin , F. Visram , W. Liu , A. Haig , J. Jiang , A. Mok , D. Lian , M.E. Wood , R. Torregrossa , M. Whiteman , I. Lobb , A. Sener

PII: S0022-5347(16)30385-8
DOI: 10.1016/j.juro.2016.05.029
Reference: JURO 13722

To appear in: *The Journal of Urology*
Accepted Date: 3 May 2016

Please cite this article as: Lin S, Visram F, Liu W, Haig A, Jiang J, Mok A, Lian D, Wood ME, Torregrossa R, Whiteman M, Lobb I, Sener A, GYY4137, a slow-releasing hydrogen sulfide donor, ameliorates renal damage associated with chronic obstructive uropathy, *The Journal of Urology*® (2016), doi: 10.1016/j.juro.2016.05.029.

GYY4137, a slow-releasing hydrogen sulfide donor, ameliorates renal damage associated with chronic obstructive uropathy

Lin, S.[1,6], Visram, F.[2,6], Liu, W.[4], Haig, A.[4], Jiang, J.[6], Mok, A.[1], Lian, D.[6], Wood, M.E.[8], Torregrossa, R.[7], Whiteman, M.[7], Lobb, I.[1,6] and Sener, A.[1,3,5,6]

[1]Department of Microbiology and Immunology, [2]Department of Physiology and Pharmacology, [3]Department of Surgery, and [4]Department of Pathology, University of Western Ontario, London, Ontario, Canada; [5]Multi-Organ Transplant Program and [6]Matthew Mailing Center for Translational Transplant Studies, London Health Sciences Center, London, Ontario, Canada; [7]University of Exeter Medical School and [8]School of Biosciences, University of Exeter, Exeter, Devon, United Kingdom

Corresponding Author: Alp Sener, MD, Ph.D., FRCSC
Department of Surgery
University of Western Ontario
University Hospital, C4-208
339 Windermere Road
London, Ontario, Canada, N6A 5A5
Tel: +1519-685-8500 x 33352
E-mail: alp.Sener@lhsc.on.ca

Word count: Abstract: 244; Text: 3000

ABSTRACT

Purpose: Chronic obstructive uropathy can cause irreversible kidney injury, atrophy, and inflammation, which can ultimately lead to fibrosis. Epithelial-mesenchymal transition (EMT) is a key trigger of fibrosis and is caused by upregulation of transforming growth factor beta 1 (TGF-β1) and angiotensin II (ANGII). Hydrogen sulfide (H_2S) is an endogenously produced gasotransmitter with cytoprotective properties. The present study aims to elucidate the effects of the slow-releasing H_2S donor GYY4137 on chronic ureteral obstruction and evaluate potential mechanisms.

Materials and Methods: Following unilateral ureteral obstruction (UUO), male Lewis rats were given daily intraperitoneal (IP) administration of phosphate buffered saline (PBS) vehicle (UUO group) or PBS+200μmol/kg GYY4137 (UUO+GYY4137 group) for 30 days. Urine and serum samples were collected to determine physiological parameters of renal function and injury. Kidneys were removed on post-operative day 30 for evaluation of histopathology and protein expression. EMT in pig kidney epithelial cells (LLC-PK1) was induced with TGF-β1 and treated with GYY4137 to evaluate potential mechanisms via *in vitro* scratch wound assays.

Results: H_2S treatment decreased serum creatinine and urine protein/creatinine excretion ratio following UUO. In addition, H_2S mitigated cortical loss, inflammatory damage, and tubulointerstitial fibrosis. Tissues exhibited decreased expression of EMT markers upon H_2S treatment. EMT progression in LLC-PK1 was alleviated upon *in vitro* administration of GYY4137.

Conclusions: Our findings demonstrate, for the first time, the protective effects of H_2S in chronic obstructive uropathy and may represent a potential therapeutic solution to ameliorate renal damage and improve clinical outcomes of urinary obstruction.

Key words: Hydrogen sulfide; Chronic obstructive uropathy; Epithelial-mesenchymal transition; Angiotensin II; Transforming growth factor β-1

INTRODUCTION

Obstructive uropathy affects approximately 10% of Americans[1]. If left untreated, it can lead to inflammation, atrophy, fibrosis, and irreversible renal injury ending in chronic kidney disease[2], which can significantly burden both patients and the health care system[3].

A proposed mechanism of obstructive uropathy postulates that injured kidney epithelial cells express cytokines that lead to leukocyte infiltration. These leukocytes subsequently release a variety of mediators such as transforming growth factor beta-1 (TGF-β1)[2]. Regulated by angiotensin II (ANGII)[4], TGF-β1 is an inducer of epithelial-mesenchymal transition (EMT), a key initiator of tissue fibrosis. Tubulointerstitial fibrosis can lead to tissue damage, loss of function and irreversible injury[5,6].

While effective surgical and non-surgical procedures are available to abrogate urinary obstruction, patients can experience long wait times between initial consultation and medical intervention, ultimately causing renal injury to accumulate. Current pharmacological treatments aimed at limiting renal injury during obstruction are scarce. Recent evidence suggests that gasotransmitters (small, endogenously-produced gaseous molecules) can exhibit anti-inflammatory and vasodilatory effects in tissue injury[7,8]. H_2S is endogenously produced by cystathionine β-synthase, cystathionine γ-lyase, and 3-mercaptopyruvate sulfurtransferase, and can mediate cellular signaling, vasodilation, apoptosis and inflammation[8].

Two recent studies have demonstrated that exogenous H_2S, released via sodium hydrosulfide (NaHS), can ameliorate damage associated with short-term ureteral obstruction[9,10]. While histopathological analyses were performed, these studies did not evaluate functional

changes. Additionally, as NaHS generates supra-physiological quantities of H_2S spontaneously in solution and has a half-life of only 15 minutes, it is a difficult potential therapeutic tool. GYY4137 is an H_2S donor molecule that allows for slow and extended release of H_2S over a 24-hour period[11]. Unlike NaHS, GYY4137 results in a sustained elevation of plasma H_2S levels upon intraperitoneal (IP) and intravenous (IV) administration[11]. GYY4137 also possesses significant anti-inflammatory, anti-oxidant and anti-apoptotic characteristics, as demonstrated by our lab and others, which makes it an ideal potential therapy against renal injury[12–15].

In the present study, we examined the effects of daily supplemental GYY4137 on serum biochemistry, glomerular function and histopathological parameters associated with a rat model of chronic unilateral ureteral obstruction (UUO)[5]. We evaluated the potential mechanisms behind our findings by examining tissue protein expression and via an *in vitro* scratch assay[16]. We demonstrate, for the first time, that exogenous H_2S treatment during chronic ureteral obstruction can preserve overall renal function, decrease inflammatory damage and attenuate fibrosis via a TGF-β1- and ANGII-mediated mechanism. Thus, H_2S supplementation is a potential therapy in the management of ureteral obstruction.

MATERIALS AND METHODS

Animal description and care

Adult male Lewis rats (250g – 300g; *Charles River Laboratories International Ltd.*) were maintained in the Animal Care and Veterinary Services facility at The University of Western Ontario (UWO) in accordance with conditions outlined by the Committee on Care and Use of Laboratory Animals of the Institute of Laboratory Animal Resources, National Research Council. The surgical protocols were approved by the Council on Animal Care and Animal Use Subcommittee of UWO.

Unilateral ureteral obstruction (UUO) procedure and postoperative monitoring

UUO is a common model used to simulate obstruction and induce fibrosis[5]. Rats were randomly divided into four groups: Sham (n=5), Sham+GYY4137 (n=5), UUO (n=8), and UUO+GYY4137 (n=7). All rats were anesthetized with ketamine and isoflurane. Sham rats underwent an abdominal incision and closure. To permanently ligate the left ureter in the UUO and UUO+GYY4137 groups, silk ties were placed across the left ureteropelvic junction. All animals were monitored for 30 days post-operatively. Animals in the UUO group were administered daily IP injections of phosphate buffered saline (PBS) vehicle (0.1 mL). UUO+GYY4137 and Sham+GYY4137 animals were given daily IP injections of GYY4137 (200 µmol/kg GYY4137 in 1 mL PBS; 1mL of PBS was required to dissolve GYY4137). GYY4137 was not dissolved in DMSO as it was being injected over an extended period of time. While this minimized toxicity, it may have limited the efficacy of the drug. On post-operative day (POD) 3, 10, 20 and 30, urine and serum samples were collected to analyze renal function. Urine protein and creatinine and serum creatinine (SCr) levels were measured using the Roche Modular P

instrument. At the time of sacrifice (POD30), kidneys were removed and divided sagittally, with each half used for either histological or quantitative real-time polymerase chain reaction (qRT-PCR) and Western Blot analysis.

Histological staining

Tissues were fixed in 10% formalin, embedded in paraffin and sectioned. Sections were stained with Masson's trichrome and terminal deoxynucleotidyl-transferase-mediated dUTP nick end labeling (TUNEL) to assess fibrosis and apoptosis, respectively. Immunohistochemical (IHC) staining with antibodies against CD68 (*Abcam*) and myeloperoxidase (MPO, *Abcam*) were used to determine macrophage and neutrophil infiltration, respectively. Sections were stained with hematoxylin and eosin (H&E) to determine cortical thickness.

Image Analysis

In a blinded fashion, TUNEL, IHC and Masson's trichrome sections were imaged using a Nikon Eclipse 90i light microscope at 10x magnification at 5 random areas. Using *ImageJ* software (*National Institutes of Health*), the number of positive cells per field of view (FOV) was quantified for TUNEL and IHC sections, and percent fibrosis per FOV was quantified for trichrome sections. Analysis of each kidney was completed using median counts of positive cells and median percent fibrosis. H&E sections were whole-slide scanned with ScanScope AT Turbo Aperio (*Leica Biosystems*); cortical thickness was measured by a blinded pathologist and normalized:

$$\text{Relative cortical thickness} = \frac{\text{Cortical thickness}}{\text{Mean cortical thickness of Sham kidneys}}$$

Quantitative RT-PCR Analysis

Using the Ambion PARIS kit (*Life Technologies*), total RNA was extracted from renal tissue and reverse transcribed into cDNA using SuperScript VILO MasterMix (*Life Technologies*) as per manufacturer's protocol. Concentrations were determined using NanoDrop 1000 Spectrophotometer (*Thermo Scientific*). qPCR was performed using Fast SYBR Green PCR Master Mix (*Life Technologies*) and analyzed using CFX96 Real Time System thermal cycler and CFX Manager Software (*Bio-rad Laboratories*). Primer sequences were designed using PrimerQuest (*Integrated DNA Technologies*) against glyceraldehyde 3-phosphate dehydrogenase (GAPDH), ANGII receptor type 1 (ANGIIR1), fibronectin, vimentin, TGF-β1, TGF-β1 receptor 2 (TGF-β1R2) and Smad2 (Table 1). GAPDH served as a reference gene, and fold-change in gene expression was calculated via the ΔΔCt method.

Western Blot Analysis

Total protein was extracted from kidney homogenate using the Ambion PARIS kit (*Life Technologies*) as per manufacturer's protocol. Lysate concentrations were quantified using the NanoDrop 1000 Spectrophotometer (*Thermo Scientific*). 30 μg of protein was separated by SDS-PAGE, transferred onto a nitrocellulose membrane and probed with antibodies against β-actin (*Santa Cruz Biotechnology*), vimentin, GAPDH and TGF-β1R2 (*GeneTex*). Secondary antibodies were Horseradish peroxidase-linked anti-rabbit or anti-mouse (*GeneTex*). Proteins were detected using ImmunStar Western C (*Bio-rad Laboratories).* Chemiluminescent signals were detected and analyzed with FluorChem M System (*Protein Simple*).

Cell culture and treatment

Pig kidney epithelial cells (LLC-PK1, *ATCC)* were cultured in Gibco Medium 199 (*Life Technologies*) supplemented with 10% fetal bovine serum and 1% penicillin/streptomycin at 37^{o}C under 5% CO_2.

In vitro scratch wound assay

In vitro scratch wound assays were performed to investigate the effects of GYY4137 on the migratory properties of EMT[16]. In 24-well plates, LLC-PK1 cells were seeded at $1.25x10^5$ cells/well, allowed to reach 90% confluency, then serum starved for 24 hours. To create a wound, the monolayer was scratched with a 200 µL micropipette tip and washed with serum-free Medium 199. Cells were treated with 10 ng/mL TGF-β1 (*Peprotech*), 10 µM GYY4137, 50 µM GYY4137, 10 ng/mL TGF-β1+10 µM GYY4137, 10 ng/mL TGF-β1+50 µM GYY4137 or untreated in serum-free Medium 199. Under standard culture conditions, the scratch wound was imaged every hour for 72 hours using IncuCyte ZOOM (*Essen Bioscience*). Area of scratch wound was quantified with *ImageJ* software (*National Institutes of Health*) and rate of migration was calculated with the following formula:

$$\text{Rate of migration} = \frac{\left(1 - \frac{\text{scratch area at 72h}}{\text{scratch area at 0h}}\right) \times 100\%}{\text{Average migration of untreated cells}}$$

Statistical Analysis

Data in figures are presented as mean ± standard error of mean (SEM). ANOVA and post-hoc Tukey's HSD were performed to determine statistical difference between multiple groups. Student's unpaired t-test was performed to determine significance at individual time points (GraphPad Prism v6.0, USA). Statistical significance was accepted at the 95% confidence interval.

RESULTS

GYY4137 treatment decreased serum creatinine and proteinuria during chronic UUO.

SCr was significantly higher on POD3 in both UUO and UUO+GYY4137 when compared to Sham ($p<0.01$, $p<0.0001$). However, SCr of UUO+GYY4137 decreased to Sham levels on POD10, whereas SCr of UUO group remained elevated until POD20 ($p<0.05$). SCr of UUO and UUO+GYY4137 remained similar to Sham on POD20 and POD30 (Figure 1A). Interestingly, urine protein to creatinine excretion ratio (UPr/Cr) of UUO group was significantly higher compared to Sham on POD3 ($p<0.05$) and remained slightly elevated until POD30, whereas the UUO+GYY4137 group demonstrated normal UPr/Cr throughout the experiment (Figure 1B). No differences in SCr and UPr/Cr were observed between Sham+GYY4137 and Sham animals (Figure 1).

GYY4137 treatment did not affect long-term apoptosis

TUNEL stain was used to determine the level of apoptosis. At POD30, all groups exhibited similar levels of apoptosis (Figure 2).

GYY4137 retained renal cortical thickness following long-term obstruction

Tissue sections were stained with H&E, and cortical thickness was measured (Figure 3A, representative images). On POD30 following UUO, there was a significant decrease in cortical thickness in both treatment groups when compared to the Sham animals ($p<0.0001$). However, the daily administration of GYY4137 was protective and led to a lesser decline in cortical thickness compared to the UUO group treated with vehicle ($p<0.05$) (Figure 3B). No difference in renal cortical thickness was observed between Sham and Sham+GYY4137 groups (Figure 3).

GYY4137 did not affect long-term inflammation

Kidney sections were immunohistochemically stained with antibodies against macrophage marker CD68 and neutrophil marker MPO. The number of CD68-positive cells in the UUO and UUO+GYY4137 were elevated compared to Sham ($p<0.01$) on POD30 (Figure 4A). There was a slight increase in neutrophil infiltration in both UUO and UUO+GYY4137 groups compared to Sham ($p=0.101$ and $p=0.515$, respectively), although the effects appeared to be slightly blunted in the UUO+GYY4137 group (Figure 4B). Sham and Sham+GYY4137 groups displayed similar levels of inflammatory infiltrate (Figure 4).

Supplemental GYY4137 mitigated renal fibrosis during chronic UUO

Fibrosis was detected through histological staining with Masson's trichrome, with fibrotic areas staining blue (Figure 5A). On POD30, there was a significant increase in the percent fibrosis of the obstructed kidney in the UUO group ($p<0.001$) which was significantly decreased to Sham levels in the UUO+GYY4137 animals ($p<0.01$) (Figure 5B). We observed no difference in renal fibrosis between Sham and Sham+GYY4137 groups (Figure 5).

GYY4137 attenuated migration associated with EMT

To assess the effect of GYY4137 on the migratory properties of EMT, a scratch wound assay was performed. Migration was determined based on the rate of wound closure and presented as a fold change relative to the control. Treatment with 10 ng/mL TGF-β1 increased migration in LLC-PK1 cells when compared to untreated control ($p=0.131$, Figure 6). TGF-β1-induced migration was significantly decreased upon treatment with 10 μM GYY4137 and 50 μM GYY4137 ($p<0.05$, Figure 6).

GYY4137 mitigated expression of EMT inducers and markers

Expression of EMT markers were determined through qRT-PCR analysis of left kidney tissue obtained at POD30. Upregulation of ANGIIR1, TGF-β1, TGF-β1R2, Smad2, Col1α1, fibronectin and vimentin were observed in both UUO and UUO+GYY4137 groups when compared to Sham. Interestingly, the UUO+GYY4137 group demonstrated a significant decrease in expression of ANGIIR1, Col1α1, fibronectin, vimentin, and Smad2 ($p<0.05$), and a marked decrease in expression of TGF-β1 and TGF-β1R2 when compared to UUO (Figure 7). Western Blot analysis at POD30 (Figure 8A) showed increased TGF-β1R2 and vimentin expression in UUO and UUO+GYY4137 groups when compared to Sham ($p=0.096$ and $p=0.100$, respectively). In keeping with the mRNA expression, both TGF-β1R2 and vimentin responses were diminished in the UUO+GYY4137 group when compared to UUO group ($p=0.478$ and $p=0.846$, respectively; Figure 8B).

DISCUSSION

Recent studies have identified H_2S as an endogenous gasotransmitter and a key modulator of physiological responses. In the kidney, H_2S plays a critical role in regulating renal function, fibrosis and inflammation[7,8,17]. Here, we examined the effects of the H_2S donor GYY4137 on a chronic model of UUO. We found that the exogenous administration of a long-acting H_2S donor alleviated tissue injury associated with chronic obstruction.

Immediately following UUO, SCr in both UUO and UUO+GYY4137 groups were significantly elevated when compared to Sham. This was unexpected, as the contralateral kidney typically compensates for the function of the obstructed kidney. However, SCr levels of UUO+GYY4137 group returned to basal levels on POD10, while SCr levels of UUO group remained elevated. Due to its vasodilatory properties, one potential explanation for these findings is based on the ability of H_2S to divert blood flow to the contralateral kidney through afferent arteriolar dilation (reno-renal reflex)[8,18]. Additionally, high doses of ketoprofen were administered on POD1 and POD2 to minimize the discomfort from complete UUO; its nephrotoxic effects were reflected in the decreased glomerular filtration rate (data not shown) in both UUO and UUO+GYY4137 groups on POD3, and UUO group only on POD10. Therefore, it is likely that the nephrotoxic properties of ketoprofen masked the early remedial effect of GYY4137. Interestingly, UUO+GYY4136 group exhibited significantly lower UPr/Cr on POD10 and slightly decreased UPr/Cr on all other PODs when compared to UUO group. As proteinuria can be seen following hyperfiltration and hypertensive injury[19], these findings demonstrate the well-established ability of H_2S to mediate intra-renal pressure[8]. Remarkably, this was also reflected in our analysis of ANGIIR1 expression on POD30, which was significantly decreased upon treatment with GYY4137. Our data not only demonstrate the detrimental effects

of UUO on overall renal function in a healthy subject, but also highlight that H_2S can mitigate renal injury by decreasing pressure in the obstructed kidney via dilation of the efferent arteriole.

The anti-apoptotic properties of H_2S have been well-documented in many previous studies[20,21]. We examined the effects of H_2S on renal apoptosis following obstruction via TUNEL staining and observed similar levels of apoptosis across all treatment groups. Previous studies have observed an acute increase in renal tubular apoptosis following UUO with a trending decline shortly thereafter, suggesting the initiation of a more fibrotic phenotype[22]. This fits well with our findings at 30 days post-UUO and highlights the importance of early decompression of the renal moiety. Future studies evaluating the reversibility of this phenotype are warranted, especially in light of our novel findings with exogenous H_2S supplementation as a potential therapeutic strategy in UUO.

H&E sections revealed a decrease in cortical thickness of UUO and UUO+GYY4137 kidneys when compared to Sham. This is attributable to tissue atrophy and nephron loss and is an indication of irreversible kidney injury[23,24]. Similar to previous studies, the administration of H_2S significantly diminished cortical loss of the obstructed kidney. However, our studies showed a more marked benefit, likely due to our use of GYY4137, a more long-acting H_2S donor compared to the sodium salts employed by other groups[10]. Our results demonstrate that exogenous H_2S may play a protective role in the face of cortical loss during chronic obstruction. Interestingly, we also observed an increase in cortical thickness of the contralateral kidney in UUO group, but not UUO+GYY4137 group, when compared to Sham. This compensatory hypertrophy of the contralateral kidney is typically observed following UUO and is often associated with hyperfiltration[23,25], which may explain the parallel increase in UPr/Cr observed

in UUO group. Our data demonstrate that GYY4137 may exert protective effects on both kidneys to alleviate renal injury.

TGF-β1 is a cytokine released by inflammatory cells and can cause fibrosis[26]. Through IHC, we examined the level of inflammatory infiltrate following UUO and found elevated levels of CD68-positive and MPO-positive cells. Although H_2S did not reduce macrophage infiltration, the slight decrease in neutrophil infiltration in UUO+GYY4137 group confirms the anti-inflammatory actions of H_2S[15,20]. Previous studies found higher levels of CD68 infiltration at higher dosages of NaHS[9], which concurred with the results obtained from our study. Additionally, CD68 is a marker for both M1 and M2 macrophages, with pro- and anti-inflammatory effects, respectively. As M2 macrophages play a critical role in kidney repair[27], increase in CD68-positive cells may therefore reflect a surge of anti-inflammatory M2 cells. UUO+GYY4137 animals also exhibited a significant decrease in fibrosis when compared to UUO group, which paralleled our inflammatory phenotype observations. Our data imply that exogenously administered H_2S can abate fibrotic injury associated with long-term obstruction, possibly through modulation of the TGF-β1/Smad pathway.

The TGF-β1/Smad pathway is regulated by ANGII, an inducer of TGF-β1 expression[4]. This pathway is a major mediator of fibrosis as it activates EMT, thereby causing epithelial cells to migrate[28]. We sought to investigate the effects of H_2S on EMT-induced migration in kidney epithelial cells using an *in vitro* scratch assay. We observed a trend towards increased migration in LLC-PK1 cells upon treatment with TGF-β1, which was attenuated upon addition of GYY4137. Echoing our *in vitro* results, we observed elevated expressions of ANGIIR1, TGF-β1 and other EMT markers in our UUO group, which were consistently alleviated upon administration of GYY4137. These trends were also reflected in our Western Blot analysis of

EMT markers, which demonstrated a marked downregulation in UUO+GYY4137 when compared to UUO. Taken together, our results imply that H_2S can mitigate renal fibrosis through attenuation of EMT.

While recent studies have demonstrated increased detrusor smooth muscle contractility upon GYY4137 administration[29], vesico-ureteral reflex was not observed in our GYY4137-treated animals. Fernandes *et al.* had administered 0.1 nM of GYY4137, therefore generating picomolar of H_2S; such minute amounts of H_2S is unlikely to induce observable effects. Additionally, they dissolved GYY4137 in dichloromethane-containing (and thus carbon monoxide-generating) DMSO[29], which may also explain this discrepancy. Furthermore, as no functional or histological differences were observed between Sham and Sham+GYY4137 groups, we conclude that daily IP administration of GYY4137 in PBS does not induce changes in a healthy kidney.

In conclusion, the administration of exogenous H_2S exerts protective effects against renal injury in a multifaceted manner. H_2S appears to alleviate renal inflammation, preserve architecture, and improve overall renal function. We have also demonstrated that GYY4137 plays a critical role in mitigating renal fibrosis by attenuating TGF-β1-induced EMT through mediating renal hypertension and ANGIIR1 expression. Our findings have important clinical implications as H_2S may be a preemptive therapy against renal damage and can ultimately improve outcomes for patients with obstructive uropathy.

ACKNOWLEDGEMENTS

This work was supported by a grant from the Lawson Health Research Foundation.

REFERENCES

1. Scales CD, Smith AC, Hanley JM, et al: Prevalence of kidney stones in the United States. Eur. Urol. 2012; **62**: 160–5. Available at: http://www.pubmedcentral.nih.gov/articlerender.fcgi?artid=3362665&tool=pmcentrez&rendertype=abstract.
2. Ucero AC, Benito-Martin A, Izquierdo MC, et al: Unilateral ureteral obstruction: beyond obstruction. Int. Urol. Nephrol. 2014; **46**: 765–76. Available at: http://www.ncbi.nlm.nih.gov/pubmed/24072452, accessed March 21, 2015.
3. Roth KS, Carter WH and Chan JCM: Obstructive Nephropathy in Children : Long-Term Progression After Relief of Posterior Urethral Valve. Pediatrics 2015; **107**: 1004–1010.
4. Liu Y: Renal fibrosis: new insights into the pathogenesis and therapeutics. Kidney Int. 2006; **69**: 213–7. Available at: http://www.ncbi.nlm.nih.gov/pubmed/16408108, accessed June 24, 2015.
5. Chevalier RL, Forbes MS and Thornhill BA: Ureteral obstruction as a model of renal interstitial fibrosis and obstructive nephropathy. Kidney Int. 2009; **75**: 1145–52. Available at: http://www.ncbi.nlm.nih.gov/pubmed/19340094, accessed December 31, 2014.
6. Tang X and Lieske JC: Acute and chronic kidney injury in nephrolithiasis. Curr. Opin. Nephrol. Hypertens. 2014; **23**: 385–90. Available at: http://www.ncbi.nlm.nih.gov/pubmed/24848936, accessed December 26, 2014.
7. Wang R: Two's company, three's a crowd: can H2S be the third endogenous gaseous transmitter? FASEB J. 2002; **16**: 1792–8. Available at: http://www.ncbi.nlm.nih.gov/pubmed/12409322.
8. Lobb I, Sonke E, Aboalsamh G, et al: Hydrogen sulphide and the kidney: Important roles in renal physiology and pathogenesis and treatment of kidney injury and disease. Nitric Oxide 2014; **46**: 55–65. Available at: http://www.ncbi.nlm.nih.gov/pubmed/25446251, accessed February 24, 2015.
9. Song K, Wang F, Li Q, et al: Hydrogen sulfide inhibits the renal fibrosis of obstructive nephropathy. Kidney Int. 2014; **85**: 1318–29. Available at: http://www.pubmedcentral.nih.gov/articlerender.fcgi?artid=4040941&tool=pmcentrez&rendertype=abstract, accessed October 7, 2014.
10. Jiang D, Zhang Y, Yang M, et al: Exogenous hydrogen sulfide prevents kidney damage following unilateral ureteral obstruction. Neurourol. Urodynamis 2014; **33**: 538–543.
11. Li L, Whiteman M, Guan YY, et al: Characterization of a novel, water-soluble hydrogen sulfide-releasing molecule (GYY4137): new insights into the biology of hydrogen sulfide. Circulation 2008; **117**: 2351–60. Available at: http://www.ncbi.nlm.nih.gov/pubmed/18443240, accessed October 14, 2014.
12. Lobb I, Mok A, Lan Z, et al: Supplemental hydrogen sulphide protects transplant kidney function and prolongs recipient survival after prolonged cold ischaemia-reperfusion injury by mitigating renal graft apoptosis and inflammation. BJU Int. 2012; **110**: E1187–95. Available at: http://www.ncbi.nlm.nih.gov/pubmed/23157304, accessed March 26, 2015.

13. Lobb I, Zhu J, Liu W, et al: Hydrogen sulfide treatment ameliorates long-term renal dysfunction resulting from prolonged warm renal ischemia-reperfusion injury. Can. Urol. Assoc. J. 2014; **8**: 413–418.

14. Lobb I, Davison M, Carter D, et al: Hydrogen sulfide treatment mitigates renal allograft ischemia reperfusion injury during cold storage and improves early transplant kidney function and survival following allogeneic renal transplantation. J. Urol. 2015.

15. Li L, Fox B, Keeble J, et al: The complex effects of the slow-releasing hydrogen sulfide donor GYY4137 in a model of acute joint inflammation and in human cartilage cells. J. Cell. Mol. Med. 2013; **17**: 365–76. Available at: http://www.pubmedcentral.nih.gov/articlerender.fcgi?artid=3823018&tool=pmcentrez&rendertype=abstract, accessed August 27, 2015.

16. Liang C-C, Park AY and Guan J-L: In vitro scratch assay: a convenient and inexpensive method for analysis of cell migration in vitro. Nat. Protoc. 2007; **2**: 329–33. Available at: http://www.ncbi.nlm.nih.gov/pubmed/17406593, accessed July 10, 2014.

17. Xia M, Chen L, Muh RW, et al: Production and Actions of Hydrogen Sulfide , a Novel Gaseous Bioactive Substance , in the Kidneys. J. Pharmacol. Exp. Ther. 2006; **329**: 1056–1062.

18. Johns EJ, Kopp UC and DiBona GF: Neural control of renal function. Compr. Physiol. 2011; **1**: 731–67. Available at: http://www.ncbi.nlm.nih.gov/pubmed/23737201, accessed August 21, 2015.

19. Helal I, Fick-Brosnahan GM, Reed-Gitomer B, et al: Glomerular hyperfiltration: definitions, mechanisms and clinical implications. Nat. Rev. Nephrol. 2012; **8**: 293–300. Available at: http://www.ncbi.nlm.nih.gov/pubmed/22349487, accessed July 2, 2015.

20. Szabó C: Hydrogen sulphide and its therapeutic potential. Nat. Rev. Drug Discov. 2007; **6**: 917–35. Available at: http://www.ncbi.nlm.nih.gov/pubmed/17948022, accessed October 17, 2014.

21. Koning AM, Frenay A-RS, Leuvenink HGD, et al: Hydrogen sulfide in renal physiology, disease and transplantation - The smell of renal protection. Nitric oxide 2015; **46**: 37–49. Available at: http://www.ncbi.nlm.nih.gov/pubmed/25656225, accessed March 25, 2015.

22. Truong LD, Petrusevska G, Yang G, et al: Cell apoptosis and proliferation in experimental chronic obstructive uropathy. Kidney Int. 1996; **50**: 200–207.

23. Ekinci S, Ciftci AO, Atilla P, et al: Ureteropelvic junction obstruction causes histologic alterations in contralateral kidney. J. Pediatr. Surg. 2003; **38**: 1650–1655. Available at: http://linkinghub.elsevier.com/retrieve/pii/S0022346803005785, accessed March 27, 2015.

24. Sugandhi N, Srinivas M, Agarwala S, et al: Effect of stem cells on renal recovery in rat model of partial unilateral upper ureteric obstruction. Pediatr. Surg. Int. 2014; **30**: 233–8. Available at: http://www.ncbi.nlm.nih.gov/pubmed/24370792, accessed March 26, 2015.

25. Metcalfe W: How does early chronic kidney disease progress? A background paper prepared for the UK Consensus Conference on early chronic kidney disease. Nephrol. Dial. Transplant. 2007; **22 Suppl 9**: ix26–30. Available at: http://www.ncbi.nlm.nih.gov/pubmed/17998229, accessed March 11, 2015.

26. Samarakoon R, Overstreet JM, Higgins SP, et al: TGF-β1 → SMAD/p53/USF2 → PAI-1 transcriptional axis in ureteral obstruction-induced renal fibrosis. Cell Tissue Res. 2012; **347**: 117–28. Available at: http://www.pubmedcentral.nih.gov/articlerender.fcgi?artid=3188682&tool=pmcentrez&rendertype=abstract, accessed March 21, 2015.

27. Kushiyama T, Oda T, Yamada M, et al: Alteration in the phenotype of macrophages in the repair of renal interstitial fibrosis in mice. Nephrology 2011; **16**: 522–535. Available at: http://doi.wiley.com/10.1111/j.1440-1797.2010.01439.x, accessed June 28, 2015.

28. Fischer KD and Agrawal DK: Vitamin D regulating TGF-ß induced epithelial-mesenchymal transition. Respir. Res. 2014; **15**: 146–159. Available at: http://www.pubmedcentral.nih.gov/articlerender.fcgi?artid=4245846&tool=pmcentrez&rendertype=abstract, accessed March 9, 2015.

29. Fernandes VS, Xin W and Petkov G V: Novel mechanism of hydrogen sulfide-induced guinea pig urinary bladder smooth muscle contraction: role of BK channels and cholinergic neurotransmission. Am. J. Physiol. Cell Physiol. 2015; **309**: C107–16. Available at: http://www.ncbi.nlm.nih.gov/pubmed/25948731, accessed February 1, 2016.

FIGURE LEGENDS

Figure 1. Exogenous GYY4137 treatment improved renal function and decreased renal injury during long-term obstruction. On post-operative days 3, 10, 20 and 30, urine and serum samples were collected from Sham (n=5), Sham + GYY4137 (n=5, 200 µmol/kg GYY4137 in 1 mL PBS, IP daily), UUO (n=8, 0.1 mL PBS, IP daily), and UUO+ GYY4137 (n=7, 200 µmol/kg GYY4137 in 1 mL PBS, IP daily) groups for analysis of A) serum creatinine levels and B) urine protein/creatinine excretion ratios (UPr/Cr). Values are normalized to body

weight on date of data collection. Data represents mean ± SEM. * $p<0.05$ compared to Sham and †$p<0.05$ compared to UUO.

Figure 2. GYY4137 treatment did not affect apoptosis following chronic UUO. Kidneys samples collected on post-operative day 30 from Sham (n=5), UUO (n=8, 0.1 mL PBS, IP daily), and UUO+GYY4137 (n=7, 200 µmol/kg GYY4137 in 1 mL PBS, IP daily) animals were stained with TUNEL. Median counts of positively stained cells per FOV at 10x magnification were determined. Each data point represents median cell count of kidney; bar represents mean.

Figure 3. Supplemental GYY4137 preserved renal cortical thickness following long-term UUO. Kidney samples were collected following Sham operations (n=5), Sham+GYY4137 (n=5, 200 µmol/kg GYY4137 in 1 mL PBS, IP daily), UUO (n=8, 0.1 mL PBS, IP daily), and UUO+GYY4137 treatment (n=7, 200 µmol/kg GYY4137 in 1 mL PBS, IP daily) at 30 days post-operation. A) Representative whole-slide scan of tissues stained with H&E. B) Cortical thickness was measured by a blinded pathologist. Measurements were normalized to mean Sham cortical thickness of the ipsilateral kidney. Values are mean ± SEM. * $p<0.05$ compared to Sham, † $p<0.05$ compared to UUO. Note: Omission of an outlier with relative cortical thickness of 0.804 in UUO.

Figure 4. GYY4137 did not decrease infiltration of inflammatory cells following chronic UUO. Kidney tissues were obtained at 30 days post-Sham (n=5), Sham+GYY4137 (n=5, 200 µmol/kg GYY4137 in 1 mL PBS, IP daily), UUO (n=8, 0.1 mL PBS, IP daily), and UUO+GYY4137 (n=7, 200 µmol/kg GYY4137 in 1 mL PBS, IP daily) for immunohistochemical analysis. A) Antibody against CD68 was used to detect presence of macrophages and B) antibody against MPO was used to detect presence of neutrophils at 10x

magnification. Positively stained cells were quantified with *ImageJ* software. Data represents mean cell count ± SEM. * $p<0.05$ compared to Sham

Figure 5. GYY4137 treatment decreased renal fibrosis following 30-day UUO. Masson's trichrome staining of kidneys 30 days after Sham (n=5), Sham+GYY4137 (n=5, 200 µmol/kg GYY4137 in 1 mL PBS, IP daily), UUO (n=8, 0.1 mL PBS, IP daily), and UUO+GYY4137 treatment (n=7, 200 µmol/kg GYY4137 in 1 mL PBS, IP daily). A) Representative images of kidneys stained for fibrotic tissue at 10x magnification. B) Median percent fibrotic area at 10x magnification was analyzed. Values are mean ± SEM. * $p<0.05$ compared to Sham, † $p<0.05$ compared to UUO.

Figure 6. GYY4137 treatment resulted decreased TGF-β1-induced migration. Scratch wound was created in a monolayer of LLC-PK1 cells in the presence of 10 ng/mL TGF-β1, 10 µM GYY4137, 50 µM GYY4137, 10 ng/mL TGF-β1+10 µM GYY317, 10 ng/mL TGF-β1+50 µM GYY417 or untreated in serum free media (n=4), and migration was observed at 0 and 72 hour post-scratch. Fold change in migration relative to untreated control cells was determined at 72 hours post-scratch. Data represents mean ± SEM. * $p<0.05$ compared to 10ng/mL TGF-β1

Figure 7. GYY4137 treatment decreased expression of genes in the epithelial-mesenchymal transition pathway. Kidney homogenates of Sham (n=3), UUO (n=3, 0.1 mL PBS, IP daily), and UUO+GYY4137 (n=3, 200 µmol/kg GYY4137 in 1 mL PBS, IP daily) were collected 30 days post-obstruction. Quantitative real-time polymerase chain reaction (qRT-PCR) analysis was performed on homogenates to determine expression of genes upstream and within the epithelial-mesenchymal transition (EMT) pathway. mRNA expressions of angiotensin II receptor type I (ANGIIR1), transforming growth factor β1 (TGF-β1), TGF-β1 receptor 2 (TGF-β1R2), Smad2,

collagen 1 alpha 1 (Col1α 1), fibronectin, and vimentin were determined. Target gene expression was normalized to GAPDH, and fold change in expression was determined relative to Sham. Data are mean ± SEM. *p<0.05 compared to Sham and †p<0.05 compared to UUO

Figure 8. Exogenous GYY4137 partially diminished expression of TGF-β1 receptor 2 and vimentin in chronic model of UUO. A) SDS-PAGE and vimentin and TGF-β1R2 Western blotting of 30 μg of kidney lysate from Sham (n=3), UUO (n=3, 0.1 mL PBS, IP daily), and UUO+GYY4137 treatment (n=3, 200 μmol/kg GYY4137 in 1 mL PBS, IP daily). GAPDH served as loading control for TGF-β1R2 blot and β-actin served as a loading control for vimentin blot. B) Chemiluminescent signals were quantified. TGF-β1R2 expression was normalized to GAPDH and vimentin expression was normalized to β-actin. Values were normalized to Sham expression of respective protein. Values are depicted in bar graph. UUO dramatically increased expression of TGF-β1R2 and vimentin, and H_2S treatment modestly decreased their expression. Data are mean ± SEM.

Table 1. qRT-PCR Primers

Genes	Primers
GAPDH	Forward: ACTCCCATTCTTCCACCTTTG Reverse: CCCTGTTGCTGTAGCCATATT
ANGIIR1	Forward: TGTCATGATCCCTACCCTCTAC Reverse: GCCACAGTCTTCAGCTTCAT
TGF-β1	Forward: CTGAACCAAGGAGACGGAATAC Reverse: GTTTGGGACTGATCCCATTGA
TGF-β1R2	Forward: CTGACCTGTTGCTGGTCATTA Reverse: GTGGACACGGTAACAGTAGAAG
Smad2	Forward: GCCTAAGTGATAGTGCGATCTT Reverse: GTTACAGCCTGGTGGGATTT
Col1α1	Forward: ACTGGTACATCAGCCCAAAC Reverse: GGAACCTTCGCTTCCATACTC
Fibronectin	Forward: CCAAGTACATTCTCAGGTGGAG Reverse: GGTCAGGCCTTTGATGGTATAG
Vimentin	Forward: CCATCAACACCGAGTTCAAGA Reverse: CGCACCTTGTCGATGTAGTT

Figure 1

A)

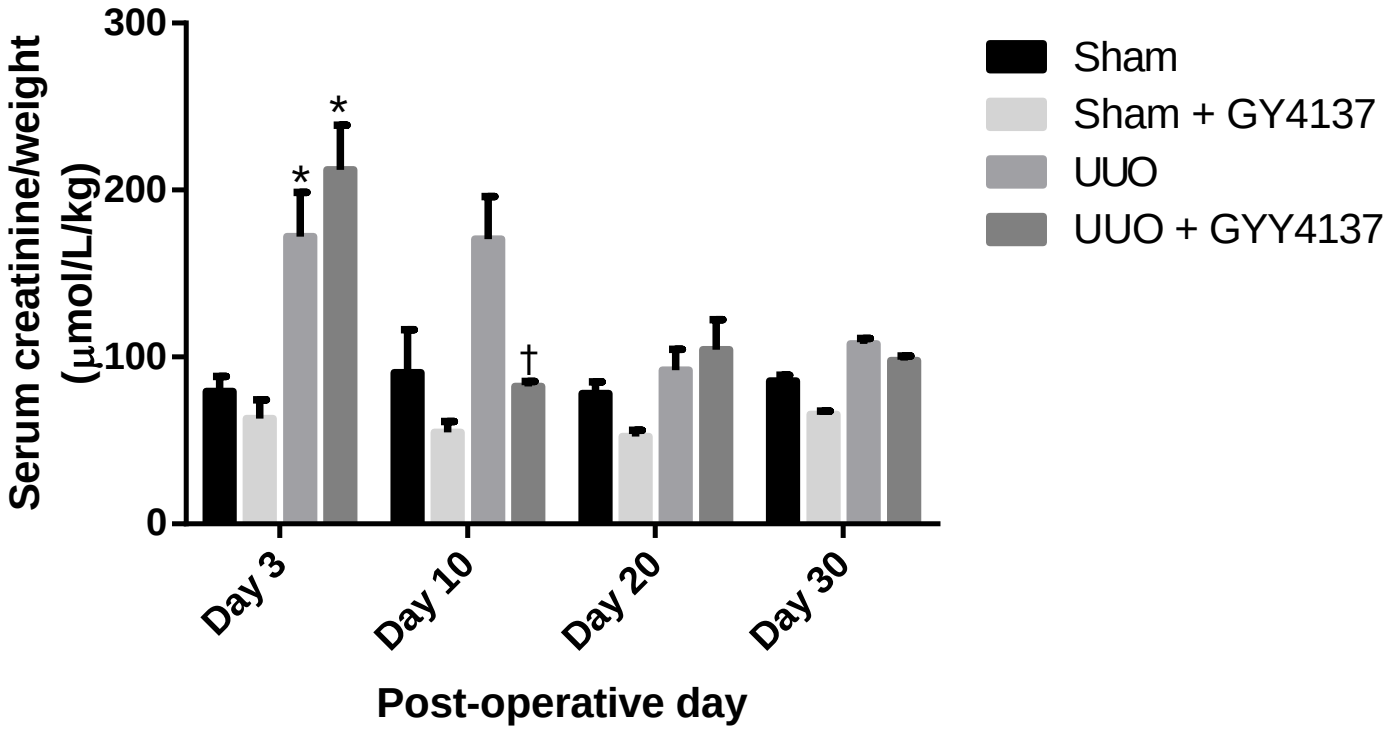
Serum creatinine/weight (µmol/L/kg)
300
200
100
0
*
*
†
Day 3
Day 10
Day 20
Day 30
Post-operative day
Sham
Sham + GY4137
UUO
UUO + GYY4137

B)

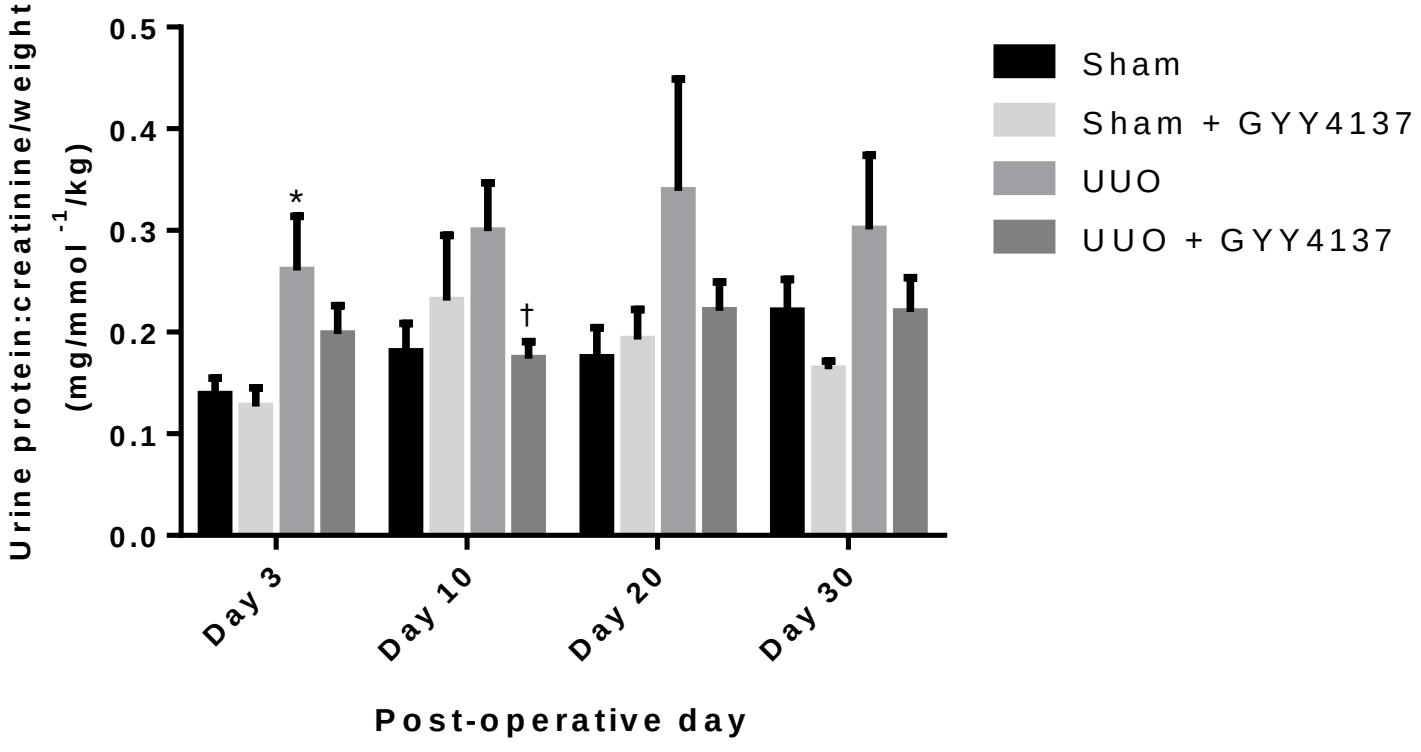
Urine protein:creatinine/weight (mg/mmol-1/kg)
0.5
0.4
0.3
0.2
0.1
0.0
*
†
Day 3
Day 10
Day 20
Day 30
Post-operative day
Sham
Sham + GYY4137
UUO
UUO + GYY4137

Figure 2

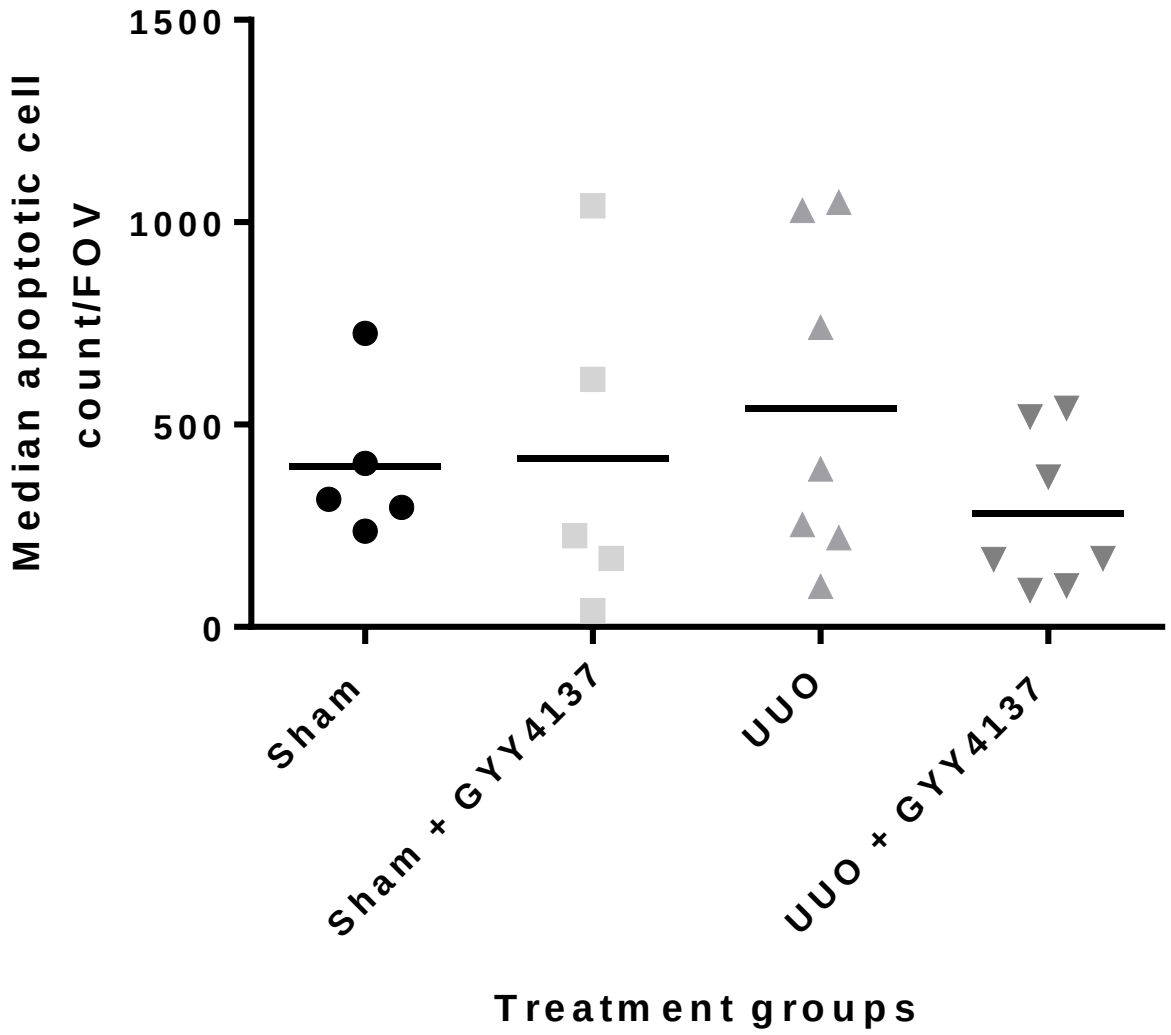
1500
1000
500
0
Median apoptotic cell count/FOV
Sham
Sham + GYY4137
UUO
UUO + GYY4137
Treatment groups

Figure 3

A)

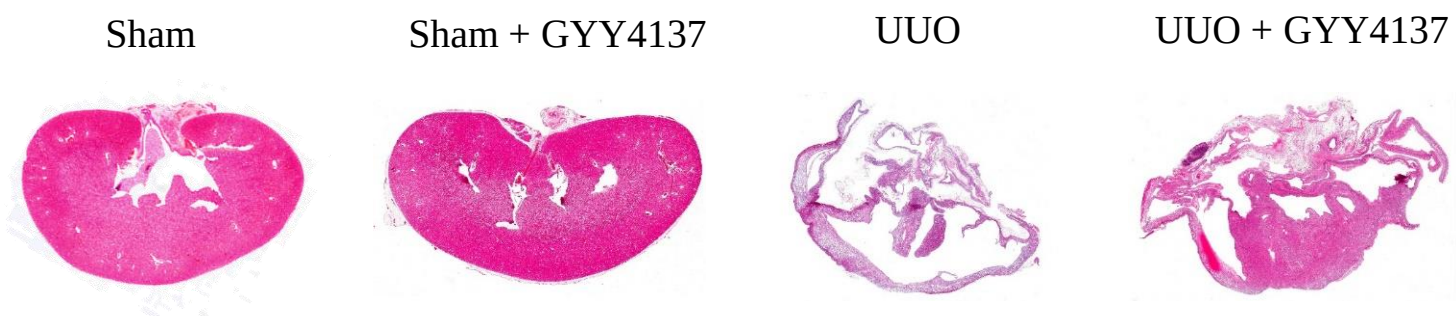
Sham
Sham + GYY4137
UUO
UUO + GYY4137

B)

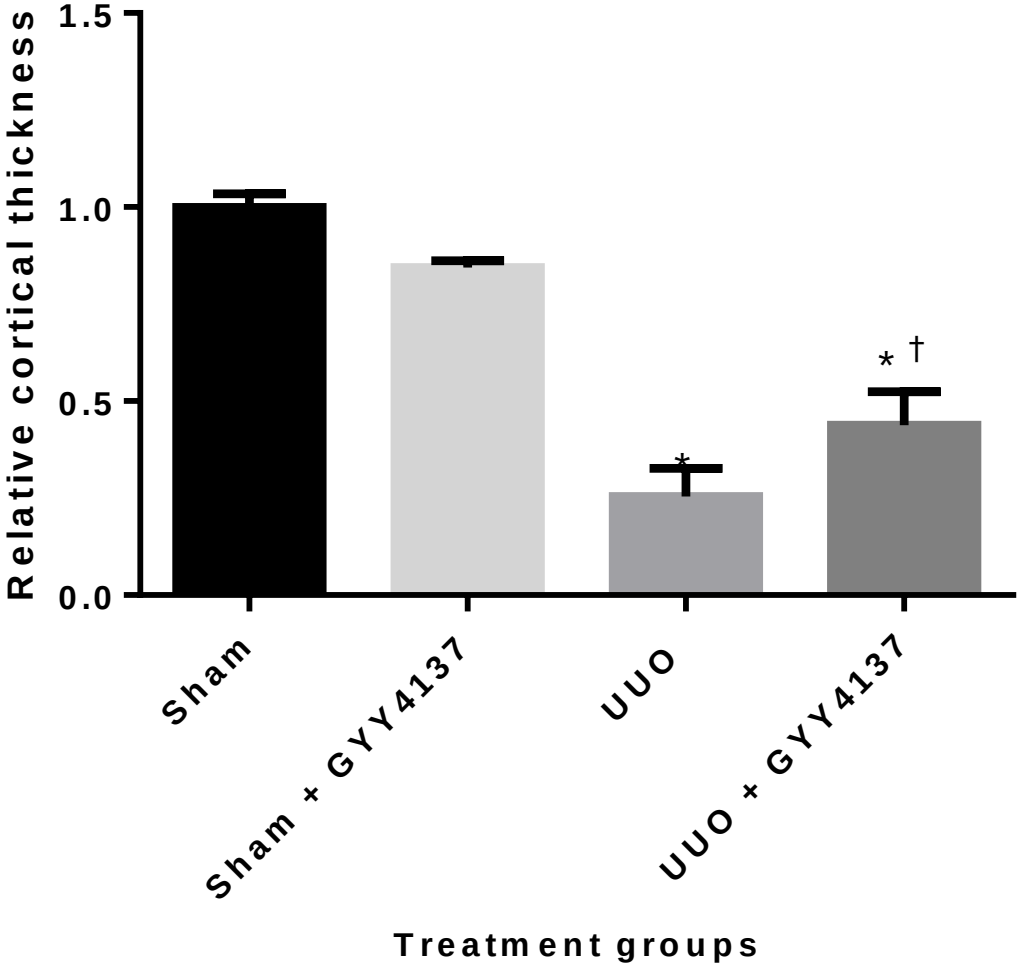
Relative cortical thickness
1.5
1.0
0.5
0.0
* †
*
Sham
Sham + GYY4137
UUO
UUO + GYY4137
Treatment groups

Figure 4

A)

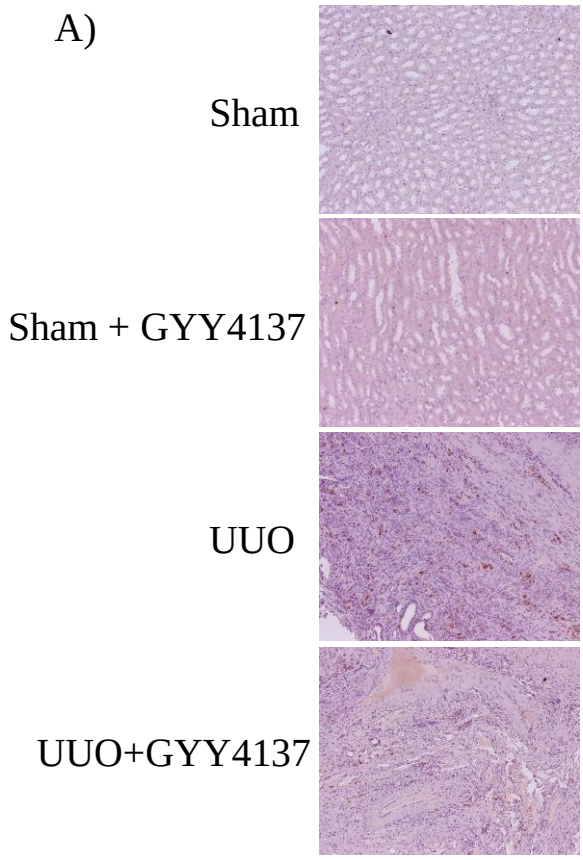
Sham
Sham + GYY4137
UUO
UUO+GYY4137

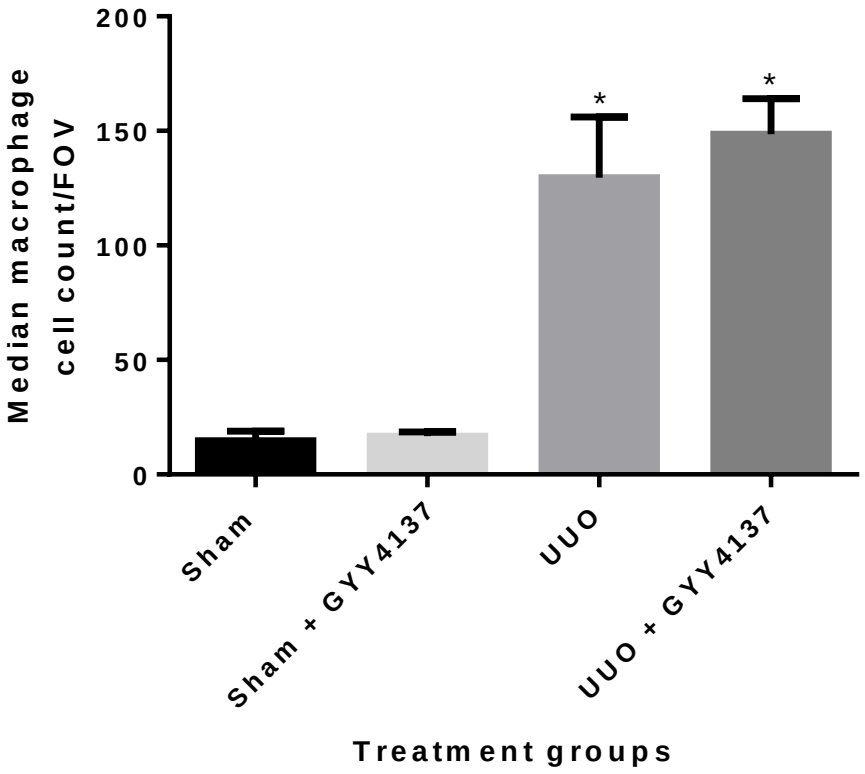
Median macrophage cell count/FOV
200
150
100
50
0
*
*
Sham
Sham + GYY4137
UUO
UUO + GYY4137
Treatment groups

B)

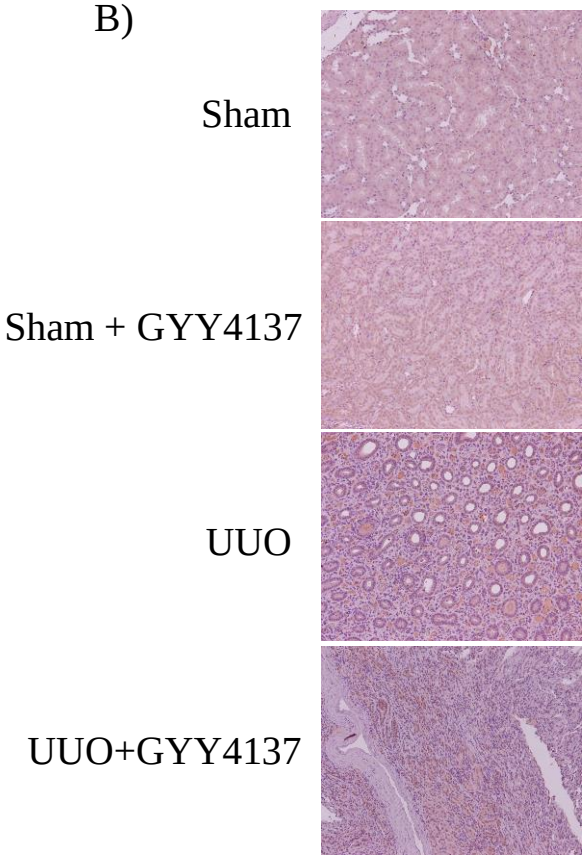
Sham
Sham + GYY4137
UUO
UUO+GYY4137

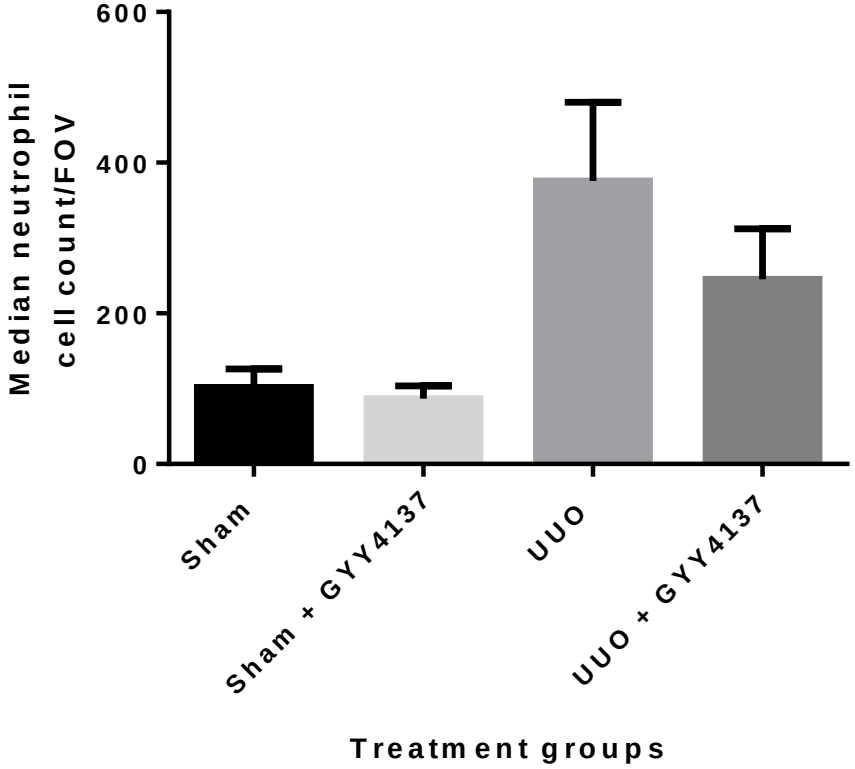
Median neutrophil cell count/FOV
600
400
200
0
Sham
Sham + GYY4137
UUO
UUO + GYY4137
Treatment groups

Figure 5

A)

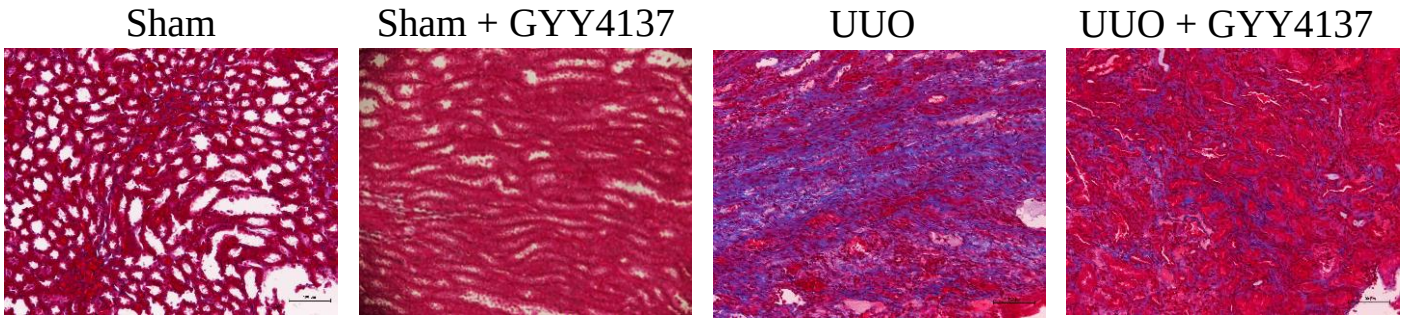
Sham
Sham + GYY4137
UUO
UUO + GYY4137

B)

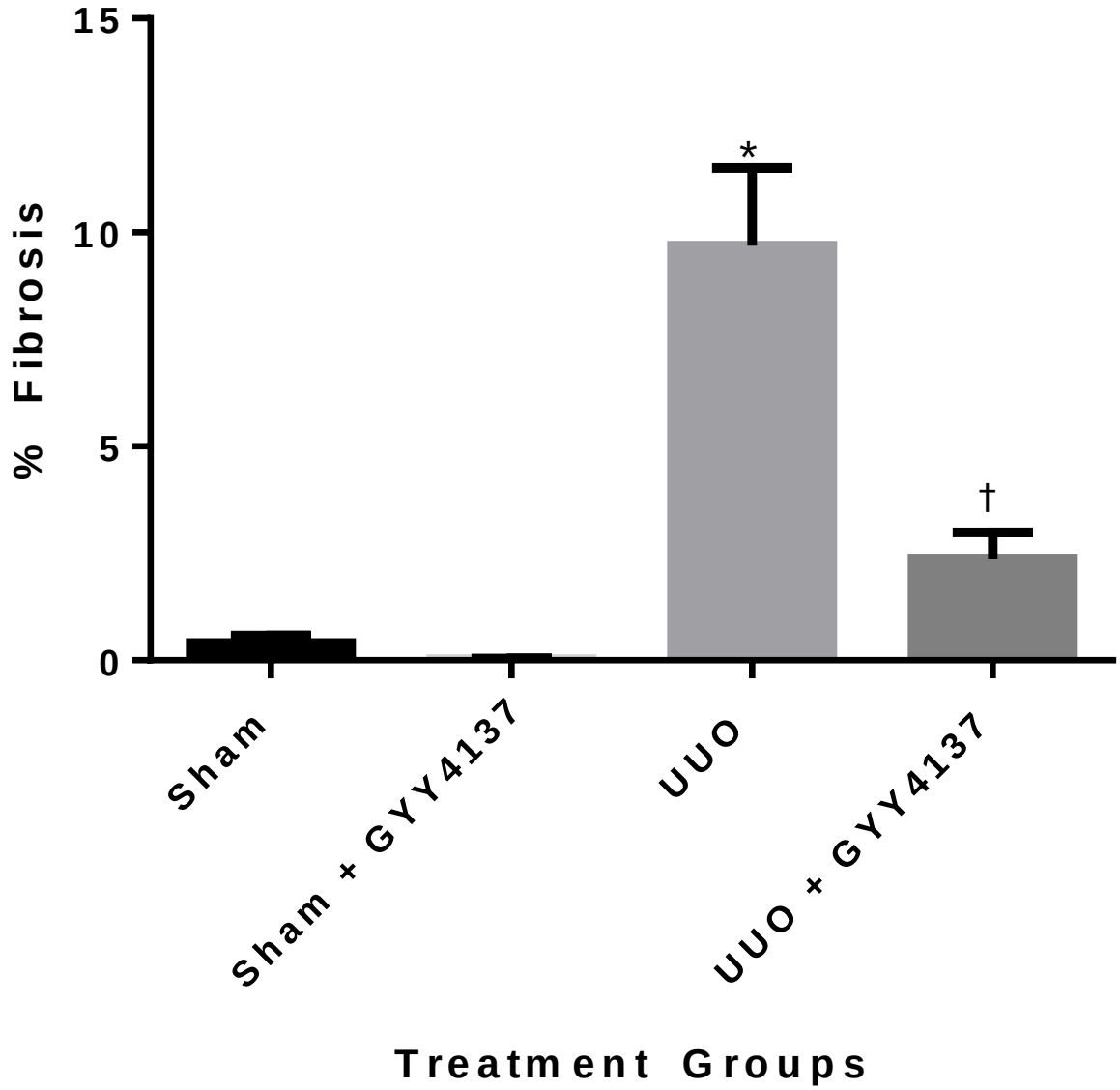
15
10
5
0
% Fibrosis
*
†
Sham
Sham + GYY4137
UUO
UUO + GYY4137
Treatment Groups

Figure 6

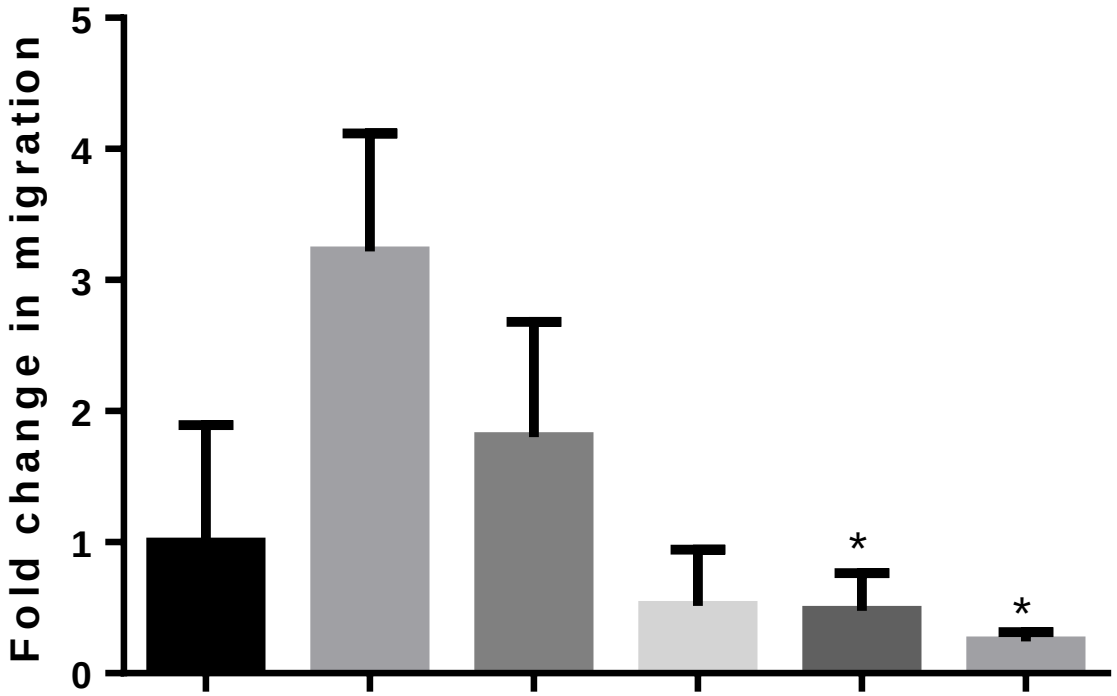

10 ng/mL TGF-β1	-	+	-	-	+	+
10 μM GYY4137	-	-	+	-	+	-
50 μM GYY4137	-	-	-	+	-	+

Figure 7

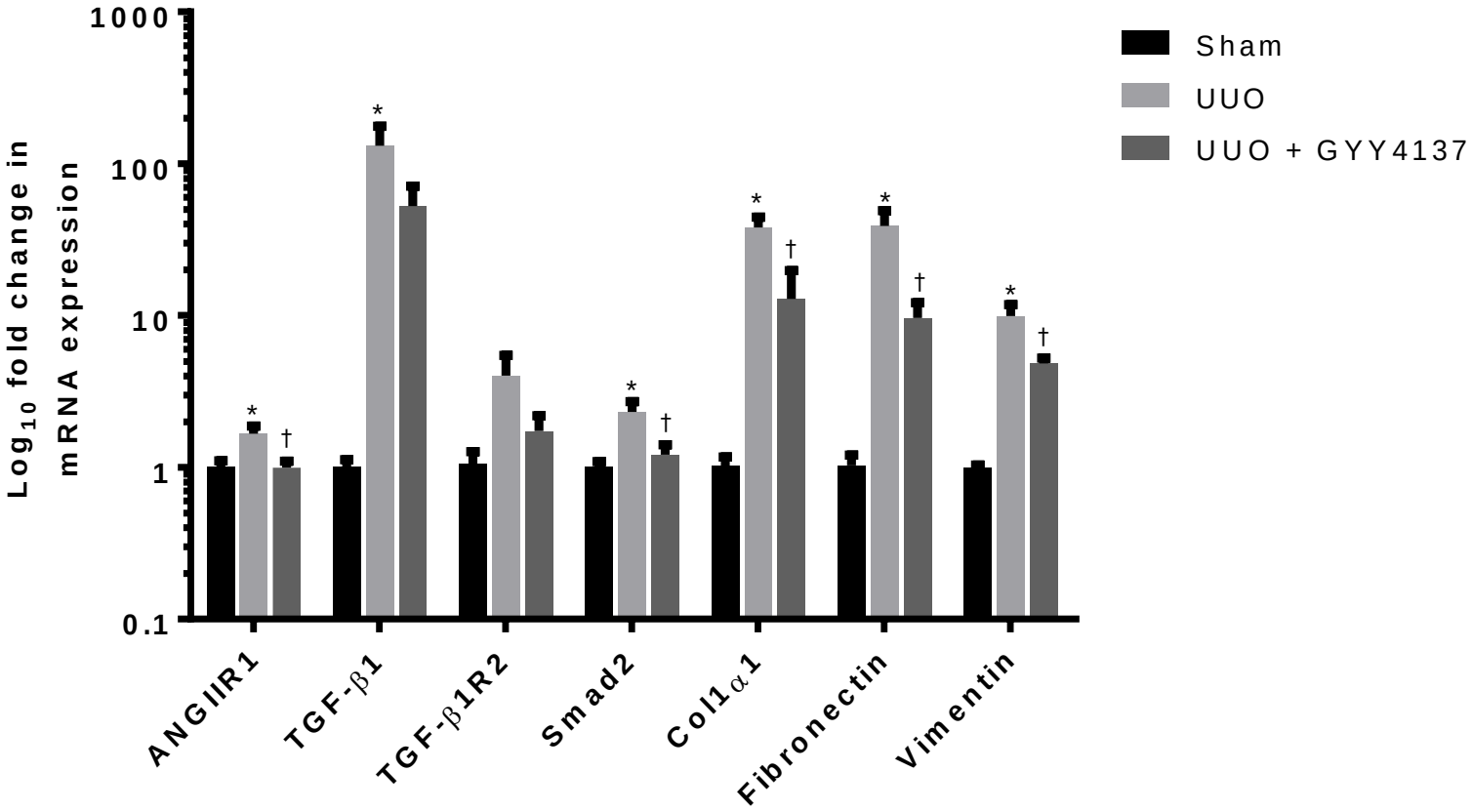
1000
100
10
1
0.1
Log10 fold change in mRNA expression
Sham
UUO
UUO + GYY4137
ANGIIR1
TGF-β1
TGF-β1R2
Smad2
Col1α1
Fibronectin
Vimentin
*
†

Figure 8

A)

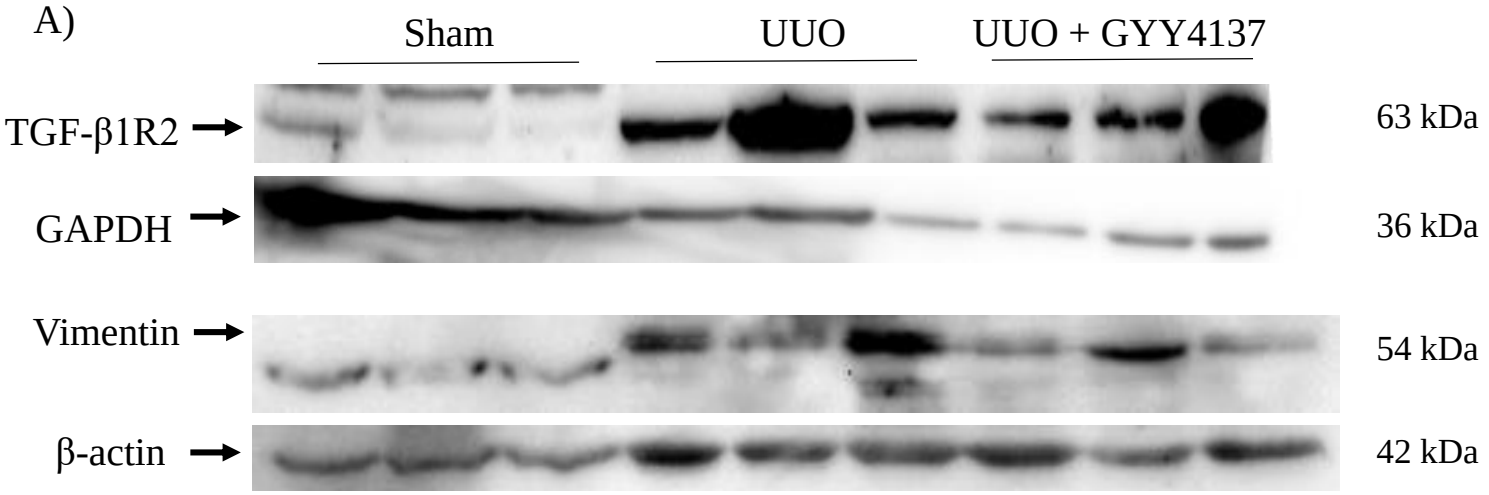
Sham
UUO
UUO + GYY4137
TGF-β1R2
GAPDH
Vimentin
β-actin
63 kDa
36 kDa
54 kDa
42 kDa

B)

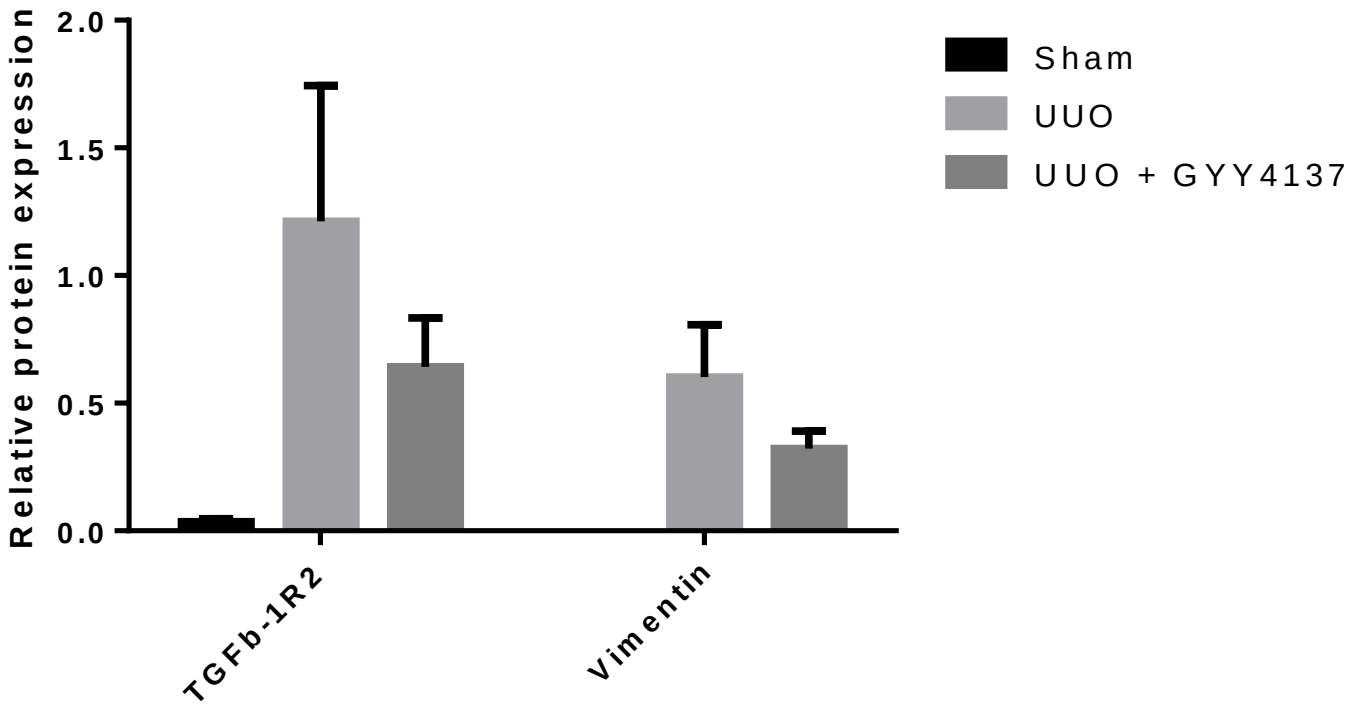
Relative protein expression
2.0
1.5
1.0
0.5
0.0
TGFb-1R2
Vimentin
Sham
UUO
UUO + GYY4137

ABBREVIATIONS

Transforming growth factor beta-1 (TGF-β1); Angiotensin II (ANGII); Epithelial-mesenchymal transition (EMT); Sodium hydrosulfide (NaSH); Intraperitoneal (IP); Intravenous (IV); Unilateral ureteral obstruction (UUO); University of Western Ontario (UWO); Phosphate buffered saline (PBS); Post-operative day (POD); quantitative real-time polymerase chain reaction (qRT-PCR); Terminal deoxynucleotidyl-transferase-mediated dUTP nick end labeling (TUNEL); Immunohistochemical (IHC); Field of view (FOV); Myeloperoxidase (MPO); Hematoxylin and eosin (H&E); Glyceraldehyde 3-phosphate dehydrogenase (GAPDH); Angiotensin II receptor type 1 (ANGIIR1); Transforming growth factor β1 receptor 2 (TGF-β1R2); Horseradish peroxidase (HRP); Gibco Medium 199 (M199); standard error of mean (SEM); Serum creatinine (SCr); Urine protein/creatinine excretion ratio (UPr/Cr);